Ion-Beam-Induced Collective Rotation of Nanocrystals

Ivo Zizak*
Berliner Elektronenspeicherring-Gesellschaft für Synchrotronstrahlung mbH, Albert-Einstein-Straße 15, 12489 Berlin, Germany

Nora Darowski, Siegfried Klaumünzer, and Gerhard Schumacher
Hahn-Meitner-Institut Berlin GmbH, Glienicker Straße 100, 14109 Berlin, Germany

Jürgen W. Gerlach
Leibniz-Institut für Oberflächenmodifizierung, Permoserstraße 15, D-04318 Leipzig, Germany

Walter Assmann
Ludwig-Maximilians-Universität München, Am Coulombwall 1, D-85748 Garching, Germany
(Received 26 November 2007; published 7 August 2008)

Vapor-deposited nanocrystalline titanium layers have been irradiated at room temperature with 350-MeV-Au ions up to 4×10^{15} Au/cm^2. Bombardment-induced texture changes were determined at the BESSY synchrotron light source. During off-normal irradiation, the nanocrystals undergo grain alignment and rotation up to ~90° at the highest ion fluence. At the same time, the whole layer exhibits shear flow very similar to that observed previously in amorphous materials. Below 1×10^{15} Au/cm^2, a reversal of the ion incidence angle leads to a back rotation of the grains. These effects are absent or immeasurably small in coarse-grained titanium but have also been found in nanocrystalline TiN and NiO. The observations can be modeled by assuming that grain boundaries behave during ion bombardment like amorphous matter or by assuming a generation of disclination dipoles moving along grain boundaries.

DOI: 10.1103/PhysRevLett.101.065503 PACS numbers: 61.80.Jh, 61.46.Hk, 68.35.−p

Nanocrystalline materials consist of polycrystals with a typical grain size d_g of a few tens of nanometers. Hence, a considerable fraction of atoms is located within grain boundaries of reduced structural order, and numerous physical and chemical properties differ significantly from those of their microcrystalline counterparts. The mechanisms of plastic deformation are of particular interest because, due to the small grain size involved, conventional operation of dislocation sources should be limited. There is experimental evidence that for $d_g > 100$ nm conventional intragrain dislocation-mediated processes prevail, whereas for $d_g < 50$ nm most of the deformation is accommodated in the grain boundaries. Several mechanisms have been proposed, among them disorder-enhanced mobility of atoms in amorphous grain boundaries, grain boundary sliding facilitated by atomic shuffling, and stress-induced formation and motion of disclination dipoles. The various deformation mechanisms are comprehensively discussed in recent reviews [1–4], but in the research community there is still widespread disagreement about their physical relevance [2]. An experimental clarification turns out to be difficult because nanocrystalline metals often deform inhomogeneously by the formation of shear bands in which the atomic structure changes continuously [1–4]. Shear banding can be avoided if, as a driving agent, the long-range stress field applied in conventional experiments is replaced by a uniform local plastic strain. In amorphous materials, such a local plastic strain is generated in the wake of fast heavy ions, and it is easily possible to achieve homogeneous strains of the order of 100% [5–7]. In this Letter, the radiation-induced deformation behavior of nanocrystalline titanium is explored. It will be shown that a surprisingly large amount of strain is brought about by the collective rotation of nanocrystals, a new effect, which is absent or immeasurably small in microcrystalline matter. It will be argued that grain rotation can be understood by a radiation-induced movement of amorphous grain boundary matter, in which the nanograins are floating, or by the movement of disclination dipoles along grain boundaries.

In the following, we use a Cartesian coordinate system with its origin in the layer-substrate interface, the z axis parallel to the surface normal, and the x axis along the projection of the ion beam onto the surface. Θ denotes the angle between the ion beam and the z axis.

Nanocrystalline titanium has been chosen because ion track effects are most pronounced in this metal [8]. 2–5 μm thick layers were deposited by physical vapor deposition on polished silicon (100) substrates of about $8 \times 8 \times 0.3$ mm^3 in size. The concentrations of gaseous impurities in the deposited layers were $\ll$0.1 at. % N, <0.1 at. % C, and <0.3 at. % O. The layers consist of nanocrystalline α-Ti with a pronounced (101) fiber texture (see Fig. 1). The samples were irradiated at 300 K with 350 MeV Au ions at $\Theta = \Theta_\Omega = 30° \pm 2°$. The irradiations were performed at the cyclotron of the Ionen-Strahl-Labor of the Hahn-Meitner-Institute. According to calculated stopping power and range of ions in matter with SRIM2003 [9], S_e is 34 keV/nm in the titanium

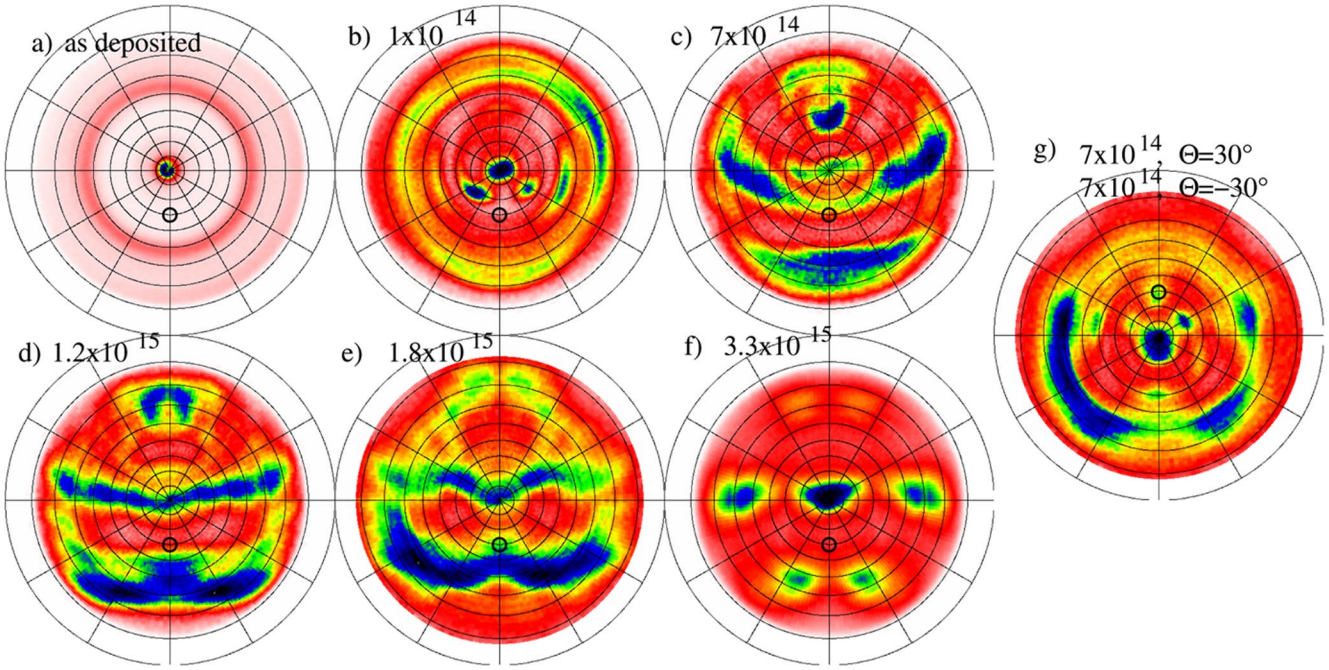

FIG. 1 (color online). Measured pole figures. (a) α-Ti (101) pole figure of the nonirradiated layer. (b)–(g) Combined pole figures of (110) and (101) planes in the nanocrystalline Ti layer at various fluences as indicated in the corner of the corresponding pole figure. Black circles mark the direction of the incident ion beam. After 18×10^{14} ions/cm^2, the texture rotated by about 60° upwards. Although the rings resulting from cylindrical symmetry are still observable, the breaking of this symmetry has already started. (f) After 33×10^{14} ions/cm^2, the texture rotation stopped, and a mosaic texture (narrow angular distribution around a preferred orientation) showing the symmetry of the hexagonal lattice is visible. Now the (110) lattice planes are parallel to the surface. (g) Test for the reversibility of the rotation. The sample from (c) was rotated 180° around the surface normal and irradiated with the same fluence, bringing the symmetry axis back to the original position within ±10°.

layers, and the ions are deeply implanted into substrate, which can be considered as radiation-resistant for the purposes of this work. Beam scanning ensured uniform irradiation of the samples with a flux of 4×10^{10} Au/cm^2 s. The samples were irradiated with fluences up to 4×10^{15} Au/cm^2 in several fractions. After each irradiation step, the orientation of the crystalline grains, i.e., the texture, was measured using Bragg diffraction of 8.05 keV x rays at the KMC2 beam line at BESSY synchrotron light source. The diffractometer was equipped with a position-sensitive detector allowing the simultaneous measurement of several Bragg reflections, including background scattering between the reflections. Peak position and shape were extracted from the measured data. The average grain sizes were estimated from the line widths using the Debye-Scherrer formula.

It is well known that, during bombardment with fast heavy ions, α-Ti transforms into ω-Ti [10,11]. Under the irradiation conditions of this work, this transformation is virtually complete at an ion fluence of 1×10^{14} Au/cm^2. The α-ω transformation leads to a starting grain size of 30 nm. (101) and (110) pole figures of ω-Ti are shown in Figs. 1(b)–1(f). The direction of the ion beam is marked with a black circle. Because the Bragg angles for (101) and (110) reflections of the ω phase differ by less than 1°, they appear simultaneously in each pole figure. The concentric rings in Fig. 1(b) are due to the (101) fiber texture inherited from the fiber texture of the original α-Ti [Fig. 1(a)]. Between 1×10^{14} and 1.8×10^{15} Au/cm^2 [Figs. 1(b)–1(e)], a rotation of the texture pattern can be seen. Simultaneously, the structure of the rings changes: The texture transforms from a fiber into a mosaic texture. At 3.3×10^{15} Au/cm^2, there is no trace of the original fiber texture left [Fig. 1(f)].

As long as the fiber texture is visible ($\Phi t < 1.8 \times 10^{15}$ Au/cm^2), the rotation of the fiber symmetry axis can be taken as a measure of the crystallite rotation. Evaluation of the pole figures shows that all crystallites rotate with the same rate around axes parallel to the y axis. The rotation angle Ω as a function of ion fluence Φt is shown in Fig. 2. For $\Phi t < 1 \times 10^{15}$ Au/cm^2, the rotation is nearly reversible. This can be demonstrated by irradiating the sample of Fig. 1(c) with additional 7×10^{14} Au/cm^2 but at an angle of $\Theta_\Omega = -30°$. The resulting texture is shown in Fig. 1(g). The fiber axis is now again oriented parallel to the surface normal as in Fig. 1(b). For $\Phi t > 1.8 \times 10^{15}$ Au/cm^2, grains having (110) planes parallel to the surface virtually stop to rotate. The rest of the grains continue to rotate until they reach the same orientation with a mosaic spread of about 20°. Concomitantly, the grain size increases from originally 30 nm to more than 150 nm at 3.3×10^{15} Au/cm^2 (limited

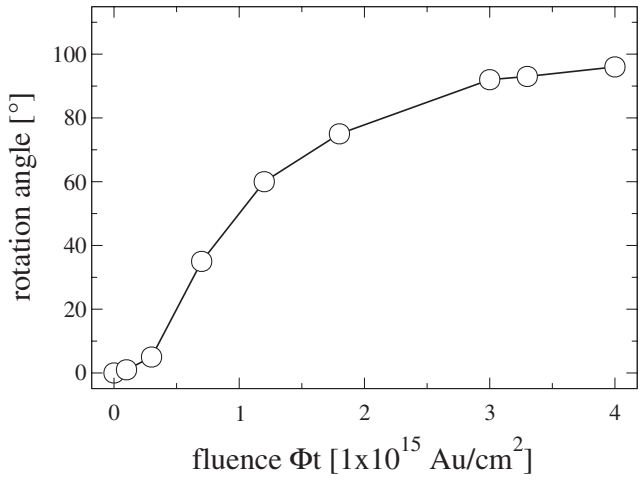

FIG. 2. Rotation angle of ω-Ti grains versus fluence.

by the resolution of the measurement). At this late stage of irradiation, no random orientation of the crystallites exists, and presumably all high-energy grain boundaries have been eliminated. In this stage, the angle of rotation is calculated as the mean value of the rotation of all grains and also plotted in Fig. 2.

The grain rotation is associated with a shear motion. This is revealed by *in situ* optical microscopy of a specimen (layer thickness $d_L = 2.7\ \mu$m, $\Theta = \Theta_{\Delta x} = 45°$) with a 20 nm thick Au grid scale at the surface. The irradiated part of the layer shifts uniformly in the positive x direction. The shift increases linearly with ion fluence and is $\Delta x = (16.5 \pm 2)\ \mu$m at a fluence of 1.5×10^{15} Au/cm^2 corresponding to an experimental shear strain $\langle \varepsilon_{xz} \rangle = \Delta x/(2d_L) \approx 3$.

At an irradiation temperature of 80 K, the grain rotation rate has the same order of magnitude as for 300 K. But grain rotation has not been seen in coarse-grained titanium (Goodfellow, $d_g > 5\ \mu$m) up to 2×10^{15} Au/cm^2. Further experiments yielded comparably large grain rotations and shear motions in nanocrystalline TiN and NiO. The weak dependence on irradiation temperature rules out an essential influence of a thermally activated motion of radiation-induced defects. The ion energy and species of this work also rule out effects of ion channeling [12,13] or implantation strain [14]. The effect is also not a remainder from the α-ω-phase transformation.

Three length scales are involved in the experiment. The first length scale is given by the radius $R_{\text{track}} \approx 3$ nm of the cylindrical region around the ion trajectory, in which material modifications are generated [15]. At a fluence increment of 3×10^{14} Au/cm^2 (cf. the abscissa of Fig. 2), a grain with $d_g = 30$ nm is, on the average, hit by more than 2000 ions, and about 80 tracks are overlapping; i.e., materials modification can be considered as uniform within the grains. The second length scale is set by d_g. Grain rotation reveals that the motion of matter is complicated on this scale. The third length scale is given by a macroscopic scale, e.g., d_L. Volume averages on this length scale, in the following denoted as $\langle \cdots \rangle$, comprise many grains and grain boundaries, and, due to the uniform energy deposition, the average strains and stresses are uniform. On this scale, quasistatic equilibrium in combination with a traction-free and planar surface implies $\langle \sigma_{xz} \rangle = 0$; i.e., there is no long-range stress field which can drive the observed shear strain $\langle \varepsilon_{xz} \rangle$. Rather, a strain associated with the direction of the ion beam must be the cause. Assuming linearity between stress and strain (implying $\langle \sigma_{ij} \rangle$ sufficiently small in comparison with the relevant elastic moduli) and ignoring volume changes, the constitutive equation must read [6,7,16,17]

$$\langle \dot{\boldsymbol{\varepsilon}} \rangle = \frac{d}{dt}(\boldsymbol{S}\langle \boldsymbol{\sigma} \rangle) + \langle A \rangle \Phi(\boldsymbol{\delta} - 3\boldsymbol{u} \otimes \boldsymbol{u}) + \boldsymbol{k}\Phi\langle \hat{\boldsymbol{\sigma}} \rangle, \qquad (1)$$

where $\langle \dot{\boldsymbol{\varepsilon}} \rangle = 1/2(\boldsymbol{\nabla} \otimes \boldsymbol{v} + (\boldsymbol{\nabla} \otimes \boldsymbol{v})^T)$ is the strain rate tensor, with $\boldsymbol{v}$ denoting the velocity of an average volume element, $\langle \boldsymbol{\sigma} \rangle$ and $\langle \hat{\boldsymbol{\sigma}} \rangle$ the average stress tensor and its deviator, respectively, $\boldsymbol{\delta}$ the unit tensor, and $\boldsymbol{u}$ the unit vector in the beam direction. The first term on the right-hand side is the material time derivative of Hooke's law with the average elastic compliance tensor $\boldsymbol{S}$. The term with the average deformation yield $\langle A \rangle$ and ion flux Φ describes the strain set by the beam in the absence of stress. The third term with the fluidity tensor $\boldsymbol{k}\Phi$ describes the modification of the second term in the presence of stress. For the boundary conditions of this work, Eq. (1) has the stationary solution

$$\boldsymbol{v}(z) = (v_x, v_y, v_z) = (6\langle A \rangle \Phi z \cos\Theta \sin\Theta, 0, 0). \qquad (2)$$

After an irradiation time t, the surface of the layer is shifted in the x direction by $\Delta x = 6\langle A \rangle \Phi t d_L \sin\Theta \cos\Theta$.

For a further analysis, we assume two limiting and idealized cases. In scenario 1, it is assumed that the plastic strain originates from the grain boundaries and the nanograins do not deform plastically. In order to maintain contiguity of the material, the nanograins have to move with an average velocity $\boldsymbol{v}$ given by Eq. (2), and they rotate with $\dot{\Omega} = 1/2\boldsymbol{\nabla} \times \boldsymbol{v}$. This scenario predicts a value of $\langle \boldsymbol{\varepsilon}_{\boldsymbol{xz}} \rangle / \Omega = 1.2$. For $\Phi t < 1.5 \times 10^{15}$ cm^{-2}, the experimental value is 2.7 ± 1.1. Although the grains are probably not completely free to rotate, the degree of mutual hindrance is surprisingly small. In this scenario, we have $\langle A \rangle = f A_{\text{GB}}$, where $f \approx 3\delta/d_g$ denotes the volume fraction of grain boundaries of width δ ($\approx$1 nm) and A_{GB} is the deformation yield in the grain boundaries. Using $d_g = 30$ nm, we estimate from Fig. 2 ($\Phi t < 1.5 \times 10^{15}$ cm^2) that $A_{\text{GB}} = 3 \times 10^{-14}$ cm^2. This value is within the range found for metallic glasses [5] and supports previous statements arguing for grain boundary mobilities close to those of amorphous materials [2,18]. In scenario 1, rotation and shear end when grain growth or grain coalescence lead to $f \to 0$.

In scenario 2, we assume that the plastic strain originates exclusively in the nanograins, presumably in the form of

dislocation loops. Transient stress fields in the wake of subsequent ions may induce a stream of dislocations toward the grain boundaries where pileup occurs. When the pileup stress at grain boundary triple lines exceeds a critical value, a splitting into climbing dislocations occurs, described as disclination dipoles moving along the grain boundaries, inducing both grain rotation and shear. This scenario has been theoretically introduced by Ovid'ko *et al.* [19–22]. An estimate for the shear strain [23] yields

$$\frac{\partial\langle\varepsilon_{xz}\rangle}{\partial t} = N_d \omega d_g v_d. \quad (3)$$

N_d denotes the area density of disclination dipoles, $\omega \approx 7^\circ = 0.12$ their average strength, and v_d their average speed. Assuming that all dislocations are moved by one Burgers vector b ($\approx$0.25 nm) due to an ion's transient ($\sim$10 ps) stress field of range of $3R_{\text{track}}$ [6,16,17], we have $v_d = b\pi(3R_{\text{track}})^2\Phi$. An upper limit for N_d is $N_d \approx 1/d_g^2 = 1 \times 10^{11}$ cm^{-2}, because at higher densities mutual annihilation is expected to increase rapidly. Inserting these numbers into Eq. (3) yields $\partial\langle\varepsilon_{xz}\rangle/\partial\Phi t = 2.3 \times 10^{-15}$ cm^{-2}, which is reasonably close to the experimental value of 2×10^{-15} cm^{-2}. The order of magnitude of the rotation rate of the nanograins is given by $\dot{\Omega} = \omega/t_d$, with $t_d = d_g/v_d$ the travel time for a disclination dipole to move from one triple line to the next one. As in scenario 1, shear rate and rotation rate are coupled, and the coupling factor is of the order of 1. In scenario 2, rotation and shear need not to stop simultaneously. Grain rotation would end when the dislocation arrays can pass a triple line without formation of disclination dipoles. This situation happens when the orientation of the neighboring grain allows for an easy dislocation glide. This process favors specific crystallite orientations with glide planes parallel to the substrate and the glide direction parallel to $\boldsymbol{x}$. Unfortunately, almost nothing is known about dislocation glide and climb in ω-Ti.

Scenario 1 may apply for ceramic nanocrystalline materials in which amorphous grain boundaries have been observed by transmission electron microscopy [24]. Scenario 2 may be more appropriate for metals, where the existence of amorphous grain boundaries is still discussed controversially [1,25]. In summary, we have shown that grain rotation is an essential part of the radiation-induced plastic strain in nanocrystalline materials. The findings can be explained either by grain boundaries which respond to ion bombardment like amorphous materials or by the disclination dipole model. The deformation phenomenology for nanocrystalline materials is identical with ion hammering of amorphous materials [6,7,16,17]. Thus, in contrast to what has been thought in the past, the borderline for ion-beam-induced deformation is not located between amorphous and crystalline matter but lies in the nanocrystalline region. Under specific conditions, dramatic changes in shape can occur, implying that nanocrystalline materials are not necessarily radiation-resistant.

We thank Dagmar Frischke and Axel Wenzel for their careful preparation of the titanium layers and Hans-Dieter Mieskes for stimulating discussions.

*ivo.zizak@bessy.de

[1] D. Wolf, V. Yamakov, S. R. Phillpot, A. Mukherjee, and H. Gleiter, Acta Mater. **53**, 1 (2005).
[2] M. A. Meyers, A. Mishra, and D. J. Benson, Prog. Mater. Sci. **51**, 427 (2006).
[3] H. van Swygenhofen and J. R. Weertman, Mater. Today **9**, No. 5, 24 (2006).
[4] M. Dao, L. Lu, R. J. Asaro, J. T. M. D. Hosson, and E. Ma, Acta Mater. **55**, 4041 (2007).
[5] M. D. Hou, S. Klaumünzer, and G. Schumacher, Phys. Rev. B **41**, 1144 (1990).
[6] H. Trinkaus and A. I. Ryazanov, Phys. Rev. Lett. **74**, 5072 (1995).
[7] A. Gutzmann, S. Klaumünzer, and P. Meier, Phys. Rev. Lett. **74**, 2256 (1995).
[8] A. Dunlop and D. Lesueur, Radiat. Eff. Defects Solids **126**, 123 (1993).
[9] J. F. Ziegler, J. P. Biersack, and U. Littmark, *The Stopping and Range of Ions in Solids* (Pergamon, New York, 1985).
[10] H. Dammak, A. Barbu, A. Dunlop, D. Lesueur, and N. Lorenzelli, Philos. Mag. Lett. **67**, 253 (1993).
[11] H. Dammak, A. Dunlop, and D. Lesueur, Philos. Mag. A **79**, 147 (1999).
[12] B. Rauschenbach and K. Helmig, Nucl. Instrum. Methods Phys. Res., Sect. B **42**, 216 (1989).
[13] S. Olliges, P. Gruber, A. Bardill, D. Ehrler, H. D. Carstanjen, and R. Spolenak, Acta Mater. **54**, 5393 (2006).
[14] O. Meyer and A. Azzam, Phys. Rev. Lett. **52**, 1629 (1984).
[15] H. Dammak, A. Dunlop, D. Lesueur, A. Brunelle, S. Della-Negra, and Y. Le Beyec, Phys. Rev. Lett. **74**, 1135 (1995).
[16] H. Trinkaus, Nucl. Instrum. Methods Phys. Res., Sect. B **107**, 155 (1996).
[17] H. Trinkaus, Nucl. Instrum. Methods Phys. Res., Sect. B **146**, 204 (1998).
[18] A. V. Sergueeva, N. A. Mara, and A. K. Mukherjee, J. Mater. Sci. **42**, 1433 (2007).
[19] I. A. Ovid'ko, Science **295**, 2386 (2002).
[20] I. A. Ovid'ko, Int. Mater. Rev. **50**, 65 (2005).
[21] M. Y. Gutkin, I. A. Ovid'ko, and N. V. Skiba, Acta Mater. **51**, 4059 (2003).
[22] M. Y. Gutkin and I. A. Ovid'ko, Appl. Phys. Lett. **87**, 251916 (2005).
[23] A. E. Romanov, Eur. J. Mech. A. Solids **22**, 727 (2003).
[24] A. Subramaniam, C. T. Koch, R. M. Cannon, and M. Ruhle, Mater. Sci. Eng. A **422**, 3 (2006).
[25] P. M. Derlet and H. van Swygenhoven, Phys. Rev. B **67**, 014202 (2003).